RESEARCH ARTICLE

Human Mutation

OFFICIAL JOURNAL
HGVS
HUMAN GENOME VARIATION SOCIETY
www.hgvs.org

Naturally Occurring Genetic Variants of Human Caspase-1 Differ Considerably in Structure and the Ability to Activate Interleukin-1β

Hella Luksch,[1] Michael J. Romanowski,[2†] Osvaldo Chara,[3] Victoria Tüngler,[1] Ernesto R. Caffarena,[4] Michael C. Heymann,[1] Peter Lohse,[5] Ivona Aksentijevich,[6] Elaine F. Remmers,[6] Silvana Flecks,[1] Nadine Quoos,[1] Johannes Gramatté,[1] Cathleen Petzold,[1] Sigrun R. Hofmann,[1] Stefan Winkler,[1] Frank Pessler,[1,7] Tilmann Kallinich,[8] Gerd Ganser,[9] Antje Nimtz-Talaska,[10] Ulrich Baumann,[11] Volker Runde,[12] Bodo Grimbacher,[13] Jennifer Birmelin,[13] Manfred Gahr,[1] Joachim Roesler,[1*‡] and Angela Rösen-Wolff[1‡]

[1]Department of Pediatrics, University Hospital Carl Gustav Carus, Dresden, Germany; [2]Department of Structural Biology, Sunesis Pharmaceuticals, Inc., South San Francisco, California; [3]Instituto de Física de Fluidos y Sistemas Biológicos (IFLYSIB), CONICET, University of La Plata (UNLP), 59-789 B1900BTE La Plata, Argentina; Center for Information Services and High-Performance Computing, Technische Universität Dresden, Dresden, Germany; [4]Programa de Computação Científica, Fundação Oswaldo Cruz, FIOCRUZ/MS, Manguinhos, Brazil; [5]Department of Clinical Chemistry, Ludwig-Maximilians-University, Munich, Germany; [6]Inflammatory Disease Section, NHGRI, NIH, Bethesda, Maryland; [7]Helmholtz Centre for Infection Research, Braunschweig, Germany; [8]Department for Pediatric Pneumology and Immunology, Charité Medical University of Berlin, Berlin, Germany; [9]St. Josef-Stift, Sendenhorst, Germany; [10]Kinderrheumatologie, Ärztehaus, Frankfurt/Oder, Germany; [11]Paediatric Pulmonology, Allergology and Neonatology, Hannover Medical School, Hannover, Germany; [12]Wilhelm-Anton-Hospital, Goch, Germany; [13]Centre of Chronic Immunodeficiency, University Hospital Freiburg, Freiburg, Germany

Communicated by David N. Cooper

Received 17 February 2012; accepted revised manuscript 11 July 2012.
Published online 25 July 2012 in Wiley Online Library (www.wiley.com/humanmutation).DOI: 10.1002/humu.22169

ABSTRACT: Caspase-1 (Interleukin-1 Converting Enzyme, ICE) is a proinflammatory enzyme that plays pivotal roles in innate immunity and many inflammatory conditions such as periodic fever syndromes and gout. Inflammation is often mediated by enzymatic activation of interleukin (IL)-1β and IL-18. We detected seven naturally occurring human *CASP1* variants with different effects on protein structure, expression, and enzymatic activity. Most mutations destabilized the caspase-1 dimer interface as revealed by crystal structure analysis and homology modeling followed by molecular dynamics simulations. All variants demonstrated decreased or absent enzymatic and IL-1β releasing activity in vitro, in a cell transfection model, and as low as 25% of normal ex vivo in a whole blood assay of samples taken from subjects with variant *CASP1*, a subset of whom suffered from unclassified autoinflammation. We conclude that decreased enzymatic activity of caspase-1 is compatible with normal life and does not prevent moderate and severe autoinflammation.**

Hum Mutat 34:122–131, 2013. © 2012 Wiley Periodicals, Inc.

KEY WORDS: autoinflammatory; rheumatic; procaspase; heterozygous; cytokine; homozygous

Introduction

Caspase-1, a proinflammatory protease, plays pivotal roles in common pathways of innate immunity [Raupach et al., 2006], autoinflammatory disorders, and diseases in which autoinflammation contributes to pathogenesis. These include rare diseases such as periodic fever syndromes and more common diseases such as atherosclerosis, type 2 diabetes, and gout [Dinarello, 2011; Martinon and Tschopp, 2004; McDermott, 2004]. The current model of caspase-1 activation comprises signaling via Toll-like (TLR) or pattern recognition receptors (PRR), efflux of potassium ions from stimulated cells [Franchi et al., 2007; Petrilli et al., 2007], danger signaling, inflammasome assembly [Kanneganti et al., 2006b; Martinon et al., 2006; Sutterwala et al., 2006], and proteolytic processing [Kanneganti et al., 2006a; Martinon et al., 2002]. Active caspase-1, and to a lesser extent procaspase-1, cleave precursors of IL-1β and IL-18, thereby producing their active forms. The function of IL-1β has been studied extensively [Dinarello, 2005; Fantuzzi and Dinarello, 1999] and its importance in autoinflammatory disorders is well documented. Accordingly, IL-1β antagonists are effective therapeutics in most of these disorders [Calligaris et al., 2008; Hawkins et al., 2003; Kuemmerle-Deschner et al., 2011; Simon et al., 2004].

Additional Supporting Information may be found in the online version of this article.

[†]Present address: Protein Structure Unit, Novartis Institutes for BioMedical Research, Inc., Cambridge, Massachusetts.

[‡]These authors contributed equally.

*Correspondence to: Joachim Roesler, Department of Pediatrics, University Medical Center Carl Gustav Carus, Fetscherstr. 74, 01307 Dresden, Germany. E-mail: Roeslerj@rcs.urz.tu-dresden.de

Contract grant sponsors: German Research Foundation (DFG, KFO 249, TP1, RO/471-11 and TP2, HO 4510/1-1); Federal Ministry of Education and Research (PID-NET, Project A4); Medical faculty of the University of Technology Dresden, MeDDrive33 (08/09): 60.153 to S.W., Germany; Marie Curie International Reintegration Grant, # 224894 to F.P., European Union.

Crystal structures of human caspase-1 have revealed that the enzyme is a tetramer of two symmetrically arranged dimers, each of which is composed of a p10 and a p20 subunit [Romanowski et al., 2004; Walker et al., 1994]. One p20/p10 dimer communicates with its neighbor through a set of direct and water-mediated hydrogen bonds as well as hydrophobic interactions.

Here, using crystallography, homology modeling followed by molecular dynamics simulations, and enzymatic and ex vivo cellular testing, we describe for the first time structural and functional features of naturally occurring frequent and newly discovered rare variants of caspase-1 (*CASP1*, MIM# 147678, ENSEMBL: ENSG00000137752).

Materials and Methods

The study was approved by the institutional review board, the Ethikkommission der Technischen Universität Dresden (EK54032007). Patients and/or their parents gave written informed consent to blood drawing and genetic analysis.

Materials

The following antibodies were used for Western blotting: Procaspase-1 A-19 antibody (sc-622) (Santa Cruz Biotechnology, Heidelberg, Germany) and IL-1β antibody #109-401-301 (Rockland Immunochemicals, Gilbertsville, PA). Polyethylenimine (PEI) was ordered from Sigma–Aldrich Chemie (Deisenhofen, Germany). Plasmids encoding procaspase-1 and proIL-1β were kind gifts from Prof. Jürg Tschopp, Faculté de Biologie et de Médecine, Department of Biochemistry, University of Lausanne, Switzerland. The QuikChange® Site-Directed Mutagenesis Kit from Stratagene (La Jolla, CA) was used to alter the procaspase-1 plasmid inserts as needed. IL-1α, IL-1β, IL-6, IL-8, and TNFα concentrations were measured using the BD Cytometric Bead Array from Becton Dickinson (Heidelberg, Germany).

Nucleotide and aa Numbering

Numbering of nucleotides reflects coding sequence numbering with +1 corresponding to the A of the ATG translation initiation codon. The initiation codon is codon 1. Wild-type (wt) *CASP1* and variants were numbered according to ENSEMBL: ENST00000436863.3. Variants have been submitted to the locus-specific database: http://www.LOVD.nl/CASP1.

Cloning and Expression of Human Caspase-1 Variants

DNA sequences of the large (p20; Asn120-Asp297; MW = 19,843.8 Da) and small (p10; Ala317-His404; MW = 10,243.7 Da) subunit of caspase-1 (GenBank accession number NM_033292; http://www.ncbi.nlm.nih.gov/genbank/) were produced by RT-PCR from RNA purified from THP-1 cells (ATCC TIB-202) as described previously [Fahr et al., 2006; O'Brien et al., 2005]. The large and small subunits were cloned separately into the *Eco*RI and *Nde*I sites of the pRSET B plasmid (Invitrogen, Carlsbad, CA). Codons for the amino acid substitutions identified in clinical samples were introduced into the cloned p20 and p10 cDNA sequences by site-directed mutagenesis using the QuikChange Site-Directed Mutagenesis Kit as recommended by the manufacturer.

Following verification of the identity of the altered sequences, the plasmids were transformed into BL21 Codon Plus cells for expression. Expression conditions, isolation of inclusion bodies, and renaturing in the presence of covalent caspase-1 inhibitors were described previously [Romanowski et al., 2004; Scheer et al., 2005]. For preparation of enzymatically active caspase-1, the recombinant enzymes were renatured in the absence of inhibitors. Preparations were stored at −80°C until use.

Crystallization, Data Collection, and Structure Determination (see also Supporting Information)

Crystals of the caspase-1 variants in complex with 3-[2-(2-benzyloxycarbonylamino-3-methyl-butyrylamino)-propionylamino]-4-oxo-pentanoic acid (z-VAD-FMK) were obtained by hanging-drop vapor diffusion at 4°C against a reservoir of 0.1 M PIPES pH 6.0, 75–175 mM $(NH_4)_2SO_4$, 25% PEG 2000 MME, 10 mM DTT, 3 mM NaN_3, and 2 mM $MgCl_2$. All crystals for data collection were cryoprotected in mother liquors supplemented with 20% (v/v) glycerol for 30–90 sec and immersion in liquid nitrogen.

Diffraction data were collected under standard cryogenic conditions on Beamline 5.0.1 at the Advanced Light Source (Berkeley, CA) using an ADSC Quantum 210 2-by-2 CCD array detector (the Arg240>Gln variant) or Beamline 5.0.2 using an ADSC Quantum 315 3-by-3 CCD array detector (the Asn263>Ser variant), and processed and scaled with CrystalClear from Rigaku/Molecular Structure Corporation [Pflugrath, 1999]. The structures were determined from single-wavelength native diffraction experiments by molecular replacement with *MOLREP* [Vagin and Teplyakov, 1997] using a search model from a previously determined structure (PDB ID 1sc4). The refinement of the initial solutions with *REFMAC* [Murshudov et al., 1997, 1999; Pannu et al., 1998] yielded experimental electron density maps suitable for model building with O [Jones et al., 1991]. The following residues were not visible in the electron density maps for the indicated protein–inhibitor complexes and were omitted from refinement of the final atomic models: 120–124 (the Arg240>Gln variant), and 120–131 (the Asn263>Ser variant). *PROCHECK* [Laskowski et al., 1993] revealed no disallowed (ϕ, ψ) combinations and excellent stereochemistry (see Supp. Table S1 for a summary of X-ray data and refinement statistics). All structure figures were prepared with PyMOL [DeLano, 2002].

Homology Modeling

The three-dimensional models of human caspase-1 mutants were generated using MODELLER 9v8 software [Eswar et al., 2007; Sali and Blundell, 1993]. Homology modeling was based on the X-ray diffraction acquired high-resolution crystal structure of the wt human caspase-1 in complex with 3-[2-(2-benzyloxycarbonylamino-3-methyl-butyrylamino)-propionylamino]-4-oxo-pentanoic acid (z-VAD-FMK) [Scheer et al., 2006]. The FASTA sequence and crystal structure of the template protein (accession number P29466) were extracted from UniProt data base (http://www.uniprot.org). MODELLER implements comparative protein structure modeling by satisfaction of spatial restraints derived from the sequence alignment and expressed as probability density functions (pdfs) for the features restrained [Eswar et al., 2007]. The pdfs restrain Cα–Cα distances, main-chain N–O distances, and main-chain and side-chain dihedral angles. The three-dimensional model of the protein is generated by an optimization process in which the model violates the input restraints as little as possible. This optimization procedure is a variable target function method that applies the conjugate gradients algorithm to positions of all nonhydrogen atoms [Sali and Blundell, 1993]. We developed 20 models for each caspase-1 mutant. The best model for each mutant was selected using the MODELLER objective function known as the DOPE assessment score (discrete optimized protein energy [Shen and Sali, 2006]). The molecular structures of

the predicted proteins and their overall stereochemical quality were validated using the program PROCHECK [Laskowski et al., 1993].

Molecular Dynamics Simulations

All simulations were performed with Gromacs program [Kutzner et al., 2007]. Coordinates of the wt protein and mutants were immersed in an orthorhombic SPC [van Gunsteren et al., 1983] water box of dimensions: 85 Å × 82.5 Å × 90.0 Å and energy-minimized with 5,000 steepest descent algorithm using periodic boundary conditions to fit the atomic positions to the Gromos96 (v. 53a6) force field [Oostenbrink et al., 2004]. All interatomic bonds were constrained using the LINCS algorithm. Nonbonded interactions were taken into account using the 6–12 Lennard–Jones potential using a cutoff radius of 14 Å and PME electrostatic treatment with a 10 Å radius for short-range interactions. Molecular dynamics simulations were performed in the NPT ensemble (300 K, 1 bar) with Nose–Hoover and Parrinello–Rahman baths for temperature and pressure, respectively. Periodic boundary conditions with a 2 femtosecond (fsec) time step were used throughout the simulations. The systems went forward during 1 nanosecond (nsec) restraining the protein coordinates to their initial positions by applying harmonic potential with spring constant K = 10 kJ/(mol Å) to stabilize water molecules around the protein. After an equilibration period of 10 nsec, simulations evolved freely for more 10 nsec, saving coordinates and velocities every 1 picosecond (psec) to further analyze structural features. Interactive visualization of molecular structures was carried out in PYMOL v1.3.

Cells

HEK 293T cells, which do not contain procaspase-1 or inflammasome components according to gene expression omnibus, GEO accession: GSM301581, were cultured in DMEM with 10% FCS and used in transfection experiments.

Transient Transfection of Procaspase-1 Variants in HEK 293T Cells

Expressions plasmids were transfected into HEK 293T cells using 0.5% PEI (Sigma–Aldrich, Germany). Cells were grown to 75% confluency in 24 well plates overnight and cotransfected with 50 ng of procaspase-1 and 500 ng of proIL-1β plasmids in 200 μl. Two hours later, another 200 μl of medium were added. For heterozygous simulations, cells were transfected with 25 ng of wt procaspase-1 and 25 ng of variant procaspase-1 plasmids together with 500 ng of proIL-1β. Supernatants were removed 24 hr after transfection and levels of mature IL-1β were determined using a CBA assay (Becton Dickinson). Cell lysates were analyzed by Western blot.

Caspase-1 Assay

A 0.55 μg of purified recombinant p20/p10 wt or variant caspase-1 lysates were incubated with 6 mM Ac-WEHD-AFC substrate in reaction buffer (50 mM HEPES pH 7,4; 50 mM KCl; 200 mM NaCl; 0,1% CHAPS; 10 mM DTT) for 60 min at 37°C, 40°C, or 42°C. Fluorescence was measured in a Mitras platereader LB940 from Berthold (Bad Wildbad, Germany). Values were calculated from 114 measurements.

Whole Blood Assay

A 140 μl of heparinized whole blood was plated into the wells of 96 well plates. Blood cells were stimulated with 1 μg/ml lipopolysaccharide (LPS) (Sigma–Aldrich) and 1 μg/ml muramyl dipeptide (MDP) (Sigma–Aldrich) in a final volume of 200 μl. The plates were placed on a plate shaker in a humidified incubator for 6 hr. Thereafter, 100 μl of PBS were added to each well and the plates were centrifuged (1200 × g for 5 min at room temperature). Supernatant from each well was removed and cytokine levels were analyzed using the CBA assay.

We also sequenced caspase-1 cDNA from the blood samples in both directions and saw in the electrospherograms about equal heights of the wt and the mutated bps (within the range of scatter of electrospherogram peak heights). This excluded gross differences in the amounts of wt and mutated caspase-1 transcripts.

Statistics

Differences in cytokine release in transfection experiments were evaluated statistically with the paired, one-tailed Mann–Whitney U test and for the whole blood assays the Wilcoxon signed rank test was used.

Results

Study Population, Patients, and CASP1 Variants

Samples from the patients included in this study had been sent to one of our centers because they were suspected by local physicians to suffer from autoinflammation caused by a genetic alteration in one of the genes *MEFV*, *NLRP3*, *MVK*, or *PSTPIP1* because they showed clinical symptoms compatible with disorders caused by such genetic alterations. Patients who had indeed a mutation in one of these genes were included in other studies, but excluded from this study. Patients with autoantibodies, a classical rheumatic disease, or mutation negative CINCA/NOMID were also excluded.

Samples from the remaining patients were analyzed for other mutations in components of the NLRP3 (NOD-like receptor family, pryin domain containing 3) inflammasome. Thereby, we detected several genetic variants of *CASP1* in some patients and their clinically unaffected relatives, and later in unrelated blood donors. Some variants (p.K319R, p.N263S, p.R240Q, p.R221C) were rare polymorphisms. Other variants (p.L265S, p.T267I, p.A329T), and subjects homozygous for p.R240Q and compound heterozygous for p.R240Q/K319R have not been detected before (Table 1). The systemic and local inflammatory symptoms of the six patients examined in detail for this study varied considerably, did not allow for the diagnosis of a known disease, and could not account for a new disease entity (Supp. Table S2). So far, severe infections or other signs of an immunodeficiency could not be substantiated. A second medical check-up revealed low titers of autoantibodies in only one of the patients. Most of the patients' relatives carrying the same *CASP1* variant were immunologically healthy and relatives with wt *CASP1* were always immunologically healthy.

Expression and Enzymatic Activity of the Caspase-1 Variants in Transfected Cells

We transfected HEK 293T cells with the procaspase-1 variants we found in our study population and with the caspase-1 substrate proIL-1β (Fig. 1) to determine whether the variants differed in their enzymatic activity from the wt form. Wt procaspase-1 is enzymatically weakly active, but autoprocessing to caspase-1 strongly enhances its activity.

Table 1. Overall Frequency of Caspase-1 Variants

CASP1 variant	Number of subjects[a] with the variant within a control population (% variants)	Number of patients[a,b] with the variant/total number of patients analyzed (% variants)	1000 Genomes/dbSNP NCBI www.1000genomes.org www.ncbi.nlm.nih.gov./snp (as at June 2012)
p.R221C/WT c.661C>T	0/100	1/468	rs151040610 (0.1%)
p.R240Q/WT c.719G>A	0/782	0/468	rs45617533 (0.4%)
p.R240Q/R240Q	0/782	1/468	Not detected
p. R240Q/K319R	0/782	1/468	Not detected
p.N263S/WT c.788A>G	4/782 (0.5%)	3/468 (0.9%)	rs139695105 (0.3%)
p.L265S/WT c.794T>C	0/782	1/468	Not detected
p.T267I/WT c.800C>T	0/580	1/468	Not detected
p.K319R/WT c.956A>G	10/782 (1.3%)	21/468 (5.5%)	rs61751523 (1.3–4%)
p.A329T/WT c.985G>A	0/580	1/468	One case reported in cosmic[c] COSM77418

Numbering of nucleotides reflects coding sequence numbering with +1 corresponding to the A of the ATG translation initiation codon. The initiation codon is codon 1. Wt *CASP1* and variants were numbered according to ENSEMBL: ENST00000436863.3.
[a]Family members of subjects and of patients with variants have not been included.
[b]The patients had no mutation in *MEFV*, *NLRP3*, *MVK*, or *PSTPIP1*; some healthy members of the same families also had the respective variant; healthy control subjects were of Caucasian and patients were of Caucasian and Mediterranean origin; SNPs other than the variants shown were synonymous.
[c]Reported as somatic mutation in Catalogue of Somatic Mutations in Cancer: www.sanger.ac.uk/genetics/CGP/cosmic/.

Procaspase-1 protein from the transfected variants except from the R221C and the A329T forms were strongly or moderately expressed (Fig. 1A). After transfection, the amount of mRNA of the R221C and A329T variants were comparable to the wt form as determined by quantitative RT-PCR. It is important to note that at high concentrations of wt procaspase-1 autoprocessing can occur without other components of the inflammasome because of the procaspase enzymatic activity [Ramage et al., 1995]. To discern bands that resulted from (pro)caspase-1 enzymatic activity from those that appeared for other reasons such as possible protein degradation by other cellular enzymes, we also included a synthetic active-site mutant C285A with no enzymatic capability. As indicated by a 33 kD band (Fig. 1A, boxed), autoprocessing only occurred in the wt, the R240Q, the N263S, and the K319R variants. The R240Q/K319R 50:50 double plasmid transfection, to mimic the compound heterozygous caspase-1 of one subject, and the R240Q form showed only very weak 33 kD bands indicating low enzymatic activity.

Mature IL-1β in cell lysates and supernatants demonstrated the efficiency of the enzymatic processing of the natural substrate proIL-1β and was fully concordant with the efficiency of autoprocessing (Fig. 1B and C). As a rough trend, the more frequent the variants were in the general population (Table 1), the more active they were. The N263S variant was only slightly less active than the wt form, whereas the decrease in activity was more pronounced in the K319R form. Moreover, the ability of the R240Q variant to cleave proIL-1β was very weak and the extremely rare variants (R221C, L265S, T267I, and A329T) showed no detectable enzymatic activity at all.

We excluded the possibility that the observed differences in enzymatic activity after transfection with the procaspase-1 variants were related to different levels of cell death (e.g., apoptosis or pyroptosis). Propidium iodine (PI) staining and measurement of the proapoptotic caspase-3 were the same for all transfections (Supp. Fig. S1).

In vitro Enzymatic Activity of Recombinant Caspase-1 Variants

To confirm our results and to further characterize the variants, we produced recombinant caspase-1 protein of those variants that demonstrated at least some activity in the transfection experiments (N263S, K319R, R240Q), quantified their enzymatic capability, performed crystal structure analysis, and simulated molecular dynamics.

The decreased enzymatic activity of the recombinant caspase-1 variants was consistent with their decreased activity in the transfection experiments (Table 2, compare with Fig. 1C). Note, however, that the concentrations of recombinant mature tetramer caspase-1 variants (Table 2) were always constant. In contrast, the respective mature variants after autoprocessing (Fig. 1) in the transfection experiment differed in quantity because they were derived from procaspase-1 with different autoprocessing efficiency (Fig. 1A). This accentuated the experimental readouts in Figure 1B and C.

Raising the reaction temperature decreased the enzymatic activity of the variants, possibly suggesting molecular instability. Although the wt form was only slightly less active at 42°C compared with 37°C, the R240Q variant had 70% less activity at 42°C. The N263S and K319R forms showed an intermediate activity and were also more sensitive to an increase in temperature than the wt form (Table 2).

Crystal Structure Analysis

As shown in Figure 2, the mutated amino acids of the variants R240Q, N263S, and K319R are located at the caspase-1 dimer interface. The two active sites in the functional wt tetramer (Fig. 2A) communicate with each other through a circuit of key amino acids that span the dimer interface. The center of the interface is marked by a conserved water molecule jointly held by two E390 residues from adjacent dimers (Fig. 2B).

In the wt tetramer, H-bonds formed by R240 (Fig. 2B) within the dimer (D336) and across the dimer interface (N259) are stabilized by two water molecules (not depicted) in the wt enzyme. In the variant R240Q enzyme, these H-bonds and those between N259 and N263 are lost (Fig. 2C).

H-bonds formed by N263 within the wt dimer with N259 and across the dimer interface (R240 and D336, Fig. 2B) are also stabilized by the water molecules. Elimination of several H-bonding interactions around the amino acid in position 263 in the variant N263S enzyme allows the two dimers to move away from each other subtly, which may lead to the disappearance of the conserved water molecule held by E390 (Fig. 2D).

Exchange of K319 by arginine (K319R; Fig. 2E), which is flexible, leads to H bonds either with D297 of the opposite p20 subunit or with Q379 ipsilateral. These bonds are not present in the wt enzyme (Fig. 2F).

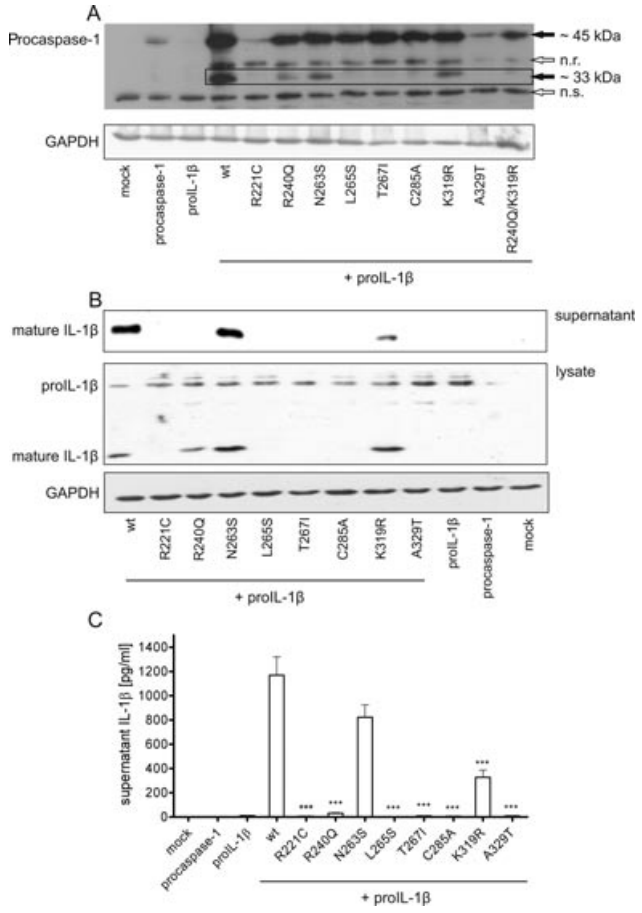

Figure 1. Expression and autoprocessing of (pro)caspase-1 variants, and proIL-1β cleavage by these variants in transfected HEK 293T cells. **A** and **B:** ProIL-1β and procaspase-1 plasmids were cotransfected. After 24 hr, supernatants and cell lysates were assayed for the presence of the respective proteins by Western blotting. Supernatants had been concentrated by methanol/chloroform precipitation. Loading control: GAPDH (glyceraldehyde-3-phosphate-dehydrogenase). **A:** Procaspase-1 variants (black arrow, 45 kDa); wt, and R240Q, N263S, and K319R variants showed an additional specific band (boxed) at approximately 33 kDa indicating autoprocessing (n.r.—not related to (pro)caspase-1 enzymatic activity; n.s.—nonspecific). **B:** Cleavage of proIL-1β by (pro)caspase-1 variants; mature IL-1β in supernatants and lysates of transfected cells. **C:** Release of mature IL-1β into the supernatant of HEK 293T cells cotransfected with proIL-1β and procaspase-1 as determined by a CBA assay. Mean and SEM, $n = 9$, $^{***}P < 0{,}001$, variant versus wt.

Homology Modeling and Molecular Dynamics Simulations of Caspase-1 Variants

On the basis of the crystallographic structure of the wt caspase-1 [Scheer et al., 2006] and the respective amino acid sequence of its variants R221C, R240Q, N263S, L265S, T267I, K319R, and A329T, the individual three-dimensional structures were calculated using homology modeling. For each variant, mutations were generated in either one or both heterodimers, and referred to as "heterozygous" and "homozygous," respectively. These variants were then employed as initial configurations for molecular dynamics simulations.

As it has been shown that dimerization via the p10·p10 interface plays a critical for protein structure and enzymatic function, we explored whether the amino acid changes of individual variants provoke geometrical alterations at the central interface of the tetramer.

Thus, the average distance between the centers of masses of the amino acids E390 located at the two opposing p10 chains (E390:E390, Fig. 3A) was calculated for the wt protein and each variant. This distance was higher in the T267I and R240Q and shorter in the R221C and K319R variants in comparison with the wt form, for both, heterozygous and homozygous tetramers. When variants L265S and A329T were substituted in only one member of the dimer pair, the distance between the two E390 amino acids was not altered, yet the distance decreased when the variant was present in both members of the dimer pair. Moreover, in the N263S variant the E390:E390 distance was decreased in the heterozygous and increased in the homozygous form of the enzyme dimer. In variants R240Q, T267I, and L265S, we found additional kinetic alterations. These variants show important fluctuations leading to metastable configurations (Fig. 3B–H).

Cytokine Production in Whole Blood Samples from Subjects with *CASP1* Variants

Following the analysis of biological activity and characterization of the correlating three-dimensional structures of caspase-1 variants, we tested the individual ability for cytokine production in an ex vivo cellular assay.

Most of our subjects encompass one variant and one wt allele, but one subject was compound heterozygous (R240Q/K319R) and another one homozygous for the R240Q allele. We first mimicked all these constellations by transfection of HEK 293T cells and then measured cytokine production in whole blood samples from all subjects available.

As shown in Figure 4A, simulated heterozygous conditions by transfection with one wt and one variant plasmid always led to less IL-1β release than transfections mimicking cells that were homozygous for the wt form. However, the results did not account for a general dominant negative effect of the variant forms because the capability of the wt caspase-1 to convert proIL-1β to active IL-1β was not suppressed by any variant form. The "compound heterozygous" R240Q/K319R cells produced less IL-1β than the respective "heterozygous" variant/wt cells and the "homozygous" R240Q cells secreted the least amounts.

Heparinized blood samples from five families with members who carry at least one variant *CASP1* allele, were stimulated with LPS and MDP. Thereafter, five cytokines (IL-1β, IL-1α, IL-8, IL-6, and TNFα)

Table 2. Enzymatic Activity of Recombinant Caspase-1 Variants with Residual Activity

Caspase-1 variant	37°C AFU	40°C AFU	42°C AFU	Decrease at 42°C compared to 37°C
Wt	33.9 ± 1.9	31.4 ± 1.3	29.1 ± 1.7	–14.1%
N263S	30.6 ± 1.2	22.5 ± 1.2	13.8 ± 2.0	–57.0%
K319R	29.5 ± 1.1	25.5 ± 1.5	17.5 ± 2.8	–41.3%
R240Q	11.2 ± 1.2	3.86 ± 0.2	3.1 ± 1.4	–73.6%

A 0.55 μg of purified recombinant p20/p10 wt or variant caspase-1 were incubated with 6 mM Ac-WEHD-AFC substrate for 60 min at different temperatures. Under these conditions, wt caspase-1 yielded a maximal substrate turnover. AFU, arbitrary fluorescence units; average of 114 measurements.

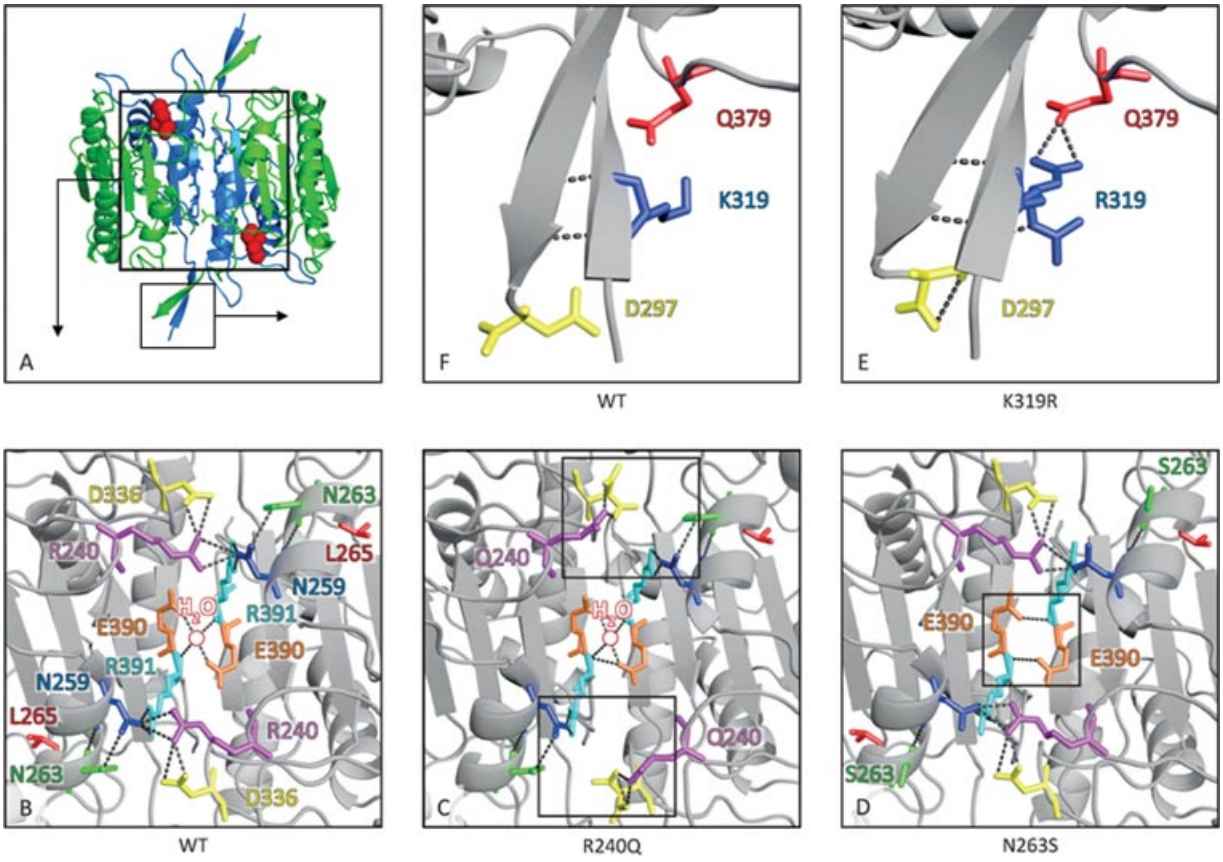

Figure 2. Structural alterations in variant caspase-1 as revealed by crystallography. **A:** Structure of the wt caspase-1 enzyme tetramer. Red: The active sites; green: p20-subunit; blue: p10-subunit. White rectangles define magnified regions of the interface as depicted in **B**–**F**. **B:** H-bonding networks around the wt caspase-1 dimer-interface residues found altered in mutated forms. H-bonds between protein atoms as well as protein atoms and water molecules are displayed as broken yellow lines. H-bonds formed by R240 within the dimer (D336) and across the dimer interface (N259), and between N263 and N259 stabilized by water molecules (not depicted) in the wt enzyme (PDB ID code 2hbq; 1.8 Å resolution). Excellent electron density for Arg240 is observed. **C:** H-bonds formed by Q240 within the dimer (D336) and across the dimer interface (N259) and to ipsilateral N263 in the R240Q variant (PDB ID code 3d6f; 1.9 Å resolution). The shorter Q240 side chain interacts with D336 within the dimer. Partially ordered electron density for the Q240 side chain indicates greater thermal motion of the side-chain atoms, especially of Q240 does not appear to participate in any other H-bonds. **D:** In the N263S variant (PDB ID code 3d6h; 2.0 Å resolution), S263 lacks the H-bonding acceptor for N259 as well as the donor for the central water molecule, which may lead to the disappearance of the conserved water molecule coordinated by E390. Excellent electron density for S263 is observed. **E:** Exchange of K319 by R319 (PDB ID code 3d6m; 1.8 Å resolution) leads to H-bonds with either D297 of the opposite p20 subunit or with the ispilateral Q379. These H-bonds are not present in the wt enzyme **F**.

were determined in the blood supernatants (plasma and medium). IL-1α and IL-1β secretion depends on caspase-1 regulated unconventional protein release. IL-8, IL-6, and TNFα were used for comparison because their release depends on conventional release mechanisms. Simultaneously drawn blood samples from family members who were homozygous for the wt *CASP1* served as control samples. Similar to the transfection model (Fig. 4A), samples from subjects with one variant allele produced significantly less IL-1β than control samples (Fig. 4B). However, blood samples from patients with one variant allele did not produce more or less IL-1β than healthy family members with the same heterozygous mutation.

In accordance with the transfection model (Fig. 4A), blood cells from the patient homozygous for R240Q (Fig. 4B filled symbol marked by *) produced less IL-1β than his heterozygous parents and brother. Also, the compound heterozygous patient (R240Q/K319R) produced less IL-1β than subjects with either R240Q/wt or K319R/wt. Due to low numbers of samples, the latter differences did not reach significance.

The amount of IL-1α released in the whole blood samples (Fig. 4C) roughly mirrored the IL-1β release (Fig. 4B). IL-1α is not activated by caspase-1, but its release from cells depends on this enzyme. Blood cells from most subjects carrying one or two variant *CASP1* alleles secreted significantly less IL-1α than cells from control samples from the same families (Fig. 4C).

We observed a trend for patient cells to release decreased amounts of IL-6 and IL-8 (R221C, R240Q/R240Q, Fig. 4D and E) or increased amounts of TNFα (L265S, A329T, Fig. 4F). However, differences in the release of these cytokines did not reach statistical significance due to the low number of samples and, therefore, it is not clear whether these differences are meaningful.

Discussion

Caspase-1 is a proinflammatory enzyme that is important in innate immunity and is of high clinical relevance. To date, little is

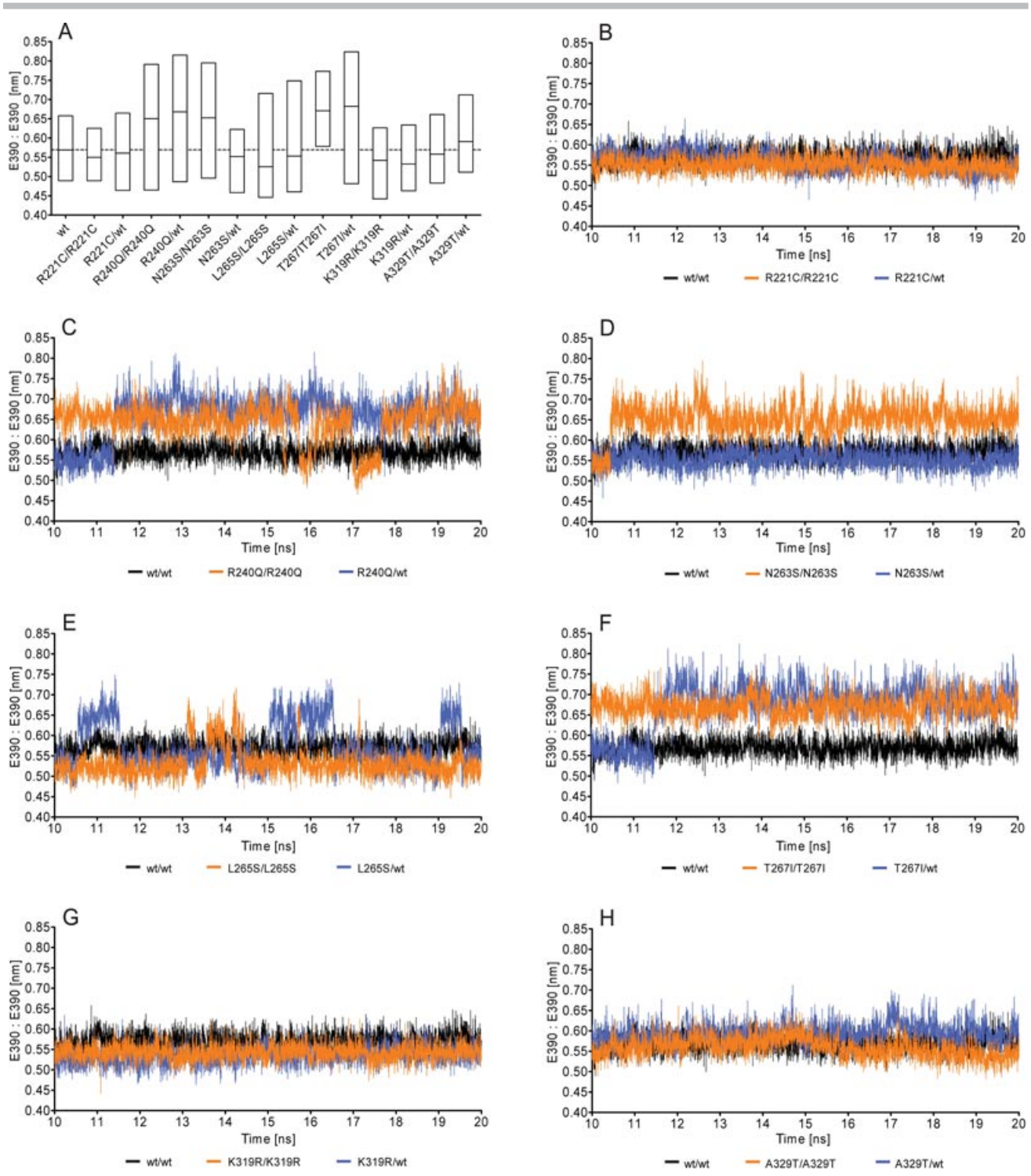

Figure 3. Distance between dimer–dimer interfaces of caspase-1 variants predicted by molecular dynamics simulations. **A:** Average distance between the centers of masses of the amino acids E390 located in the two opposing p10 chains of caspase-1 variants (E390:E390). The horizontal dashed line corresponds to the average of the E390:E390 distance in the wt caspase-1 (wt). **B–H:** Detailed time course of E390:390 distance of caspase-1 variants calculated from molecular dynamics simulations. Wt/wt, variant/variant, and variant/wt stand for "homozygous" and "heterozygous" forms of the enzyme variants, respectively.

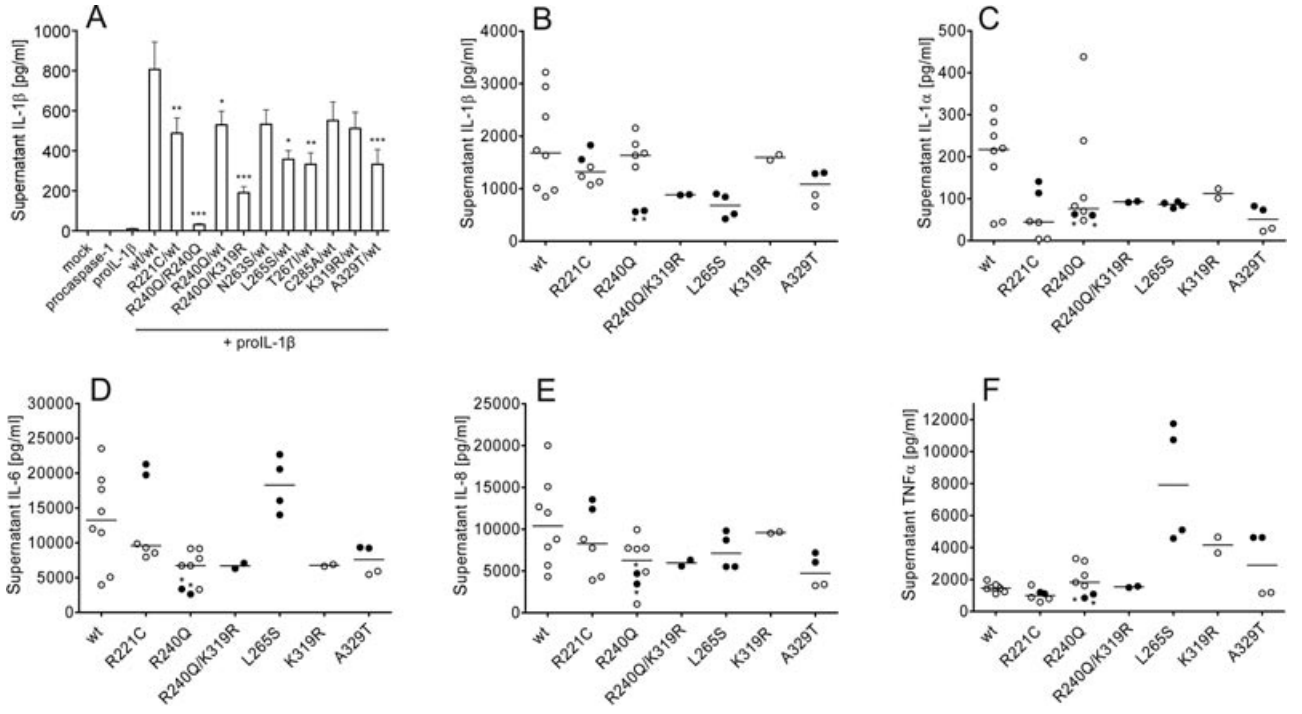

Figure 4. Cytokine secretion in whole blood samples from subjects with *CASP1* variants and from transfected cells. **A:** Release of mature IL-1β into the supernatants of HEK 293T cells cotransfected with proIL-1β and procaspase-1 variant plasmids as determined by a CBA assay. Mean and SEM of $n = 9$, $^{*}P < 0.01$, $^{**}P < 0.005$, $^{***}P < 0.001$, variant versus wt. **B–F:** Secretion of mature IL-1β, $p < 0.025$ (**B**); IL-1α, $p < 0.016$ (**C**); IL-6, n.s. (**D**); IL-8, n.s. (**E**); and TNFα, n.s. (**F**) into supernatant of LPS/MDP stimulated whole blood samples as determined by CBA assay; *P* values: all subjects with variant alleles together (12 individuals, $n = 25$ independent samples) versus family members with wt alleles only (4 relatives, $n = 8$ samples). Horizontal line: median; healthy subjects: open circles; diseased subjects: closed circles; wt: family members with wt alleles only; all subjects with *CASP1* variants were heterozygous except one diseased homozygous subject (R240Q/R240Q) indicated by asterisks, and one diseased compound heterozygous subject (R240Q/K319R).

known about types and frequencies of naturally occurring human caspase-1 variants and nothing is known about their functional features. We came across such variants while analyzing genes that encode components of the NLRP3 inflammasome in families with members suffering from yet unclassified autoinflammatory diseases.

Our data consistently show that naturally occurring caspase-1 variants differ widely from the wt form in terms of structure, stability, and enzymatic activity. The relatively frequent N263S and K319R variants (Table 1) show moderately decreased enzymatic activity (Fig. 1) and possibly decreased stability at higher temperatures (Table 2). The R240Q variant is also not extremely rare (Table 1), but demonstrates only residual autoprocessing and enzymatic activity. The very rare variants R221C, L265S, T267I, and A329T do not show any activity at all.

Caspase-1 enzymatic activity is not only responsible for cleavage of proIL-1β, but also for secretion of mature IL-1β (unconventional protein secretion [Keller et al., 2008]). The ratio of secreted IL-1β to intracellular IL-1β is decreased in the variants with residual activity compared to the wt (Fig. 1B, R240Q, N263S, K319R, compare supernatant and lysate) suggesting that secretion is even more impaired than proIL-1β cleavage.

We solved high-resolution structures of the three caspase-1 variants identified in our patients that are still enzymatically active. Homology modeling and molecular dynamics simulations allowed us to characterize not only qualitatively but quantitatively structural alterations of all caspase-1 variants. Crystallographic structures represent "homozygous" mature forms of the enzyme, in which both dimers of the functional tetramer contained the relevant amino acid alteration. Two amino acid substitutions (R240Q and N263S) destabilized, to varying degrees the dimer interface by eliminating hydrogen bond interactions that would normally hold the dimers of the functional tetramer together (Fig. 2). This result was in agreement with our molecular dynamic simulations. Distances between respective E390 amino acids, a measure of the distance between the dimers, were increased in R240Q and N263S homozygous forms of the enzyme (Fig. 3A, C, and D). As a consequence, loss of these interactions disrupted a circuit of residues that normally enables one active site of the tetramer to communicate with the other active site. In addition, analysis of the crystallographic structure of the R240Q variant indicates that this mutation may also severely alter the stability of loop 3, the largest loop of the active site, which normally undergoes a dramatic conformational change upon ligand binding [Romanowski et al., 2004]. A more detailed discussion can be found in the Supporting Information.

According to crystallography, the K319R mutation does not induce an alteration across the center of the dimer–dimer interface. This result was confirmed by molecular dynamics in which the E390:E390 is not changed in the homozygous form of the enzyme for this mutation (Fig. 3A and G). Nevertheless, it appears as if the substitution of lysine by arginine induces new hydrogen bonds between the amino acid at position 319 and both D297 and Q379 (Fig. 2F, compare with the wt in Fig. 2E). Although the dimer–dimer interface is altered in R240Q as well as in N263S (Fig. 3A, C, and D), it is not in the K319R variant (Fig. 3A and G). Conversely, only

in K319R the hydrogen bonds involving the amino acid 319 are perturbed. The fact that the three studied variants show decreased enzymatic activity (Table 2) indicates that both the dimer interface and the hydrogen bond network linked to the 319 lysine are crucial for function. Interestingly, the mutation-induced dimer separation seen in molecular dynamics simulation, particularly notable in variants R240Q, N263S and more subtle in L265S, is accompanied by a two-state oscillation (Fig. 3A, C, D, and E, respectively). These oscillations indicate the presence of two metastable configurations for the dimer–dimer interface, which is currently investigated in another study.

The ex vivo measurements using whole blood samples from subjects that carry the variant alleles, are consistent with the in vitro results and the results of the transfection experiments (Fig. 4). Monocytes and neutrophils [Mankan et al., 2011] are most probably the most important source of IL-1β (and IL-1α) in the blood samples. TNFalpha, IL-6, and IL-8, measured for comparison, are again secreted by monocytes and neutrophils, but also by other leukocytes. When stimulated with LPS and MDP, the blood samples from subjects with one variant allele produce significantly less IL-1β than samples from family members exclusively with wt alleles. The decrease in IL-1β production may even be more pronounced in samples from the homozygous R240Q subject. IL-1α production follows a pattern that resembles IL-1β production. Even though caspase-1 is not needed to activate IL-1α it is nevertheless important for its release from the cells [Keller et al., 2008]. The release of the other cytokines measured does not follow a clear consistent pattern.

As a result of preselection, approximately half of the subjects with variant caspase-1 alleles suffer from variegated symptoms that can mostly be categorized as autoinflammatory, as only one patient had low levels of autoantibodies. The other half of the subjects, parents or siblings of the patients, are immunologically healthy. Nobody shows clear signs of an immunodeficiency such as recurrent infections. Cells from the homozygous R240Q patient can still produce approximately 25% of IL-1β of a person with two wt alleles. This amount of IL-1β may be sufficient to prevent immunodeficiency. However, it is still possible that patients in consanguineous families exist that have two null alleles of *CASP1* and do suffer from an immunodeficiency because secretion of IL-1β during inflammation/infection is part of innate immunity and conserved in evolution.

The etiology of the patients' autoinflammatory disorders may vary a lot. For example, the enhanced secretion of TNFalpha only in the siblings with the L265S variant (Fig. 4F) could perhaps indicate that their pathomechanism of autoinflammation differs from that of the other patients.

It is not clear whether any relationship exists between the patients' disorders and the caspase-1 variants. Also, it is even possible that the patients would suffer from autoinflammation more severely if they could produce normal amounts of IL-1β.

As a last possibility, these hypomorphic caspase-1 variants could paradoxically contribute to inflammation. Lamkanfi and colleagues proposed a mechanism by which enzymatically inactive (pro)caspase-1 can activate NF-κB via RIP2 and could hence be proinflammatory [Lamkanfi et al., 2004]. We are currently investigating the hypothesis that this mechanism accounts for or contributes to the inflammation in the patients.

Thus, we conclude that naturally occurring genetic variants of human caspase-1 differ considerably in structure and ability to activate IL-1β and that strongly decreased production of IL-1β (and IL-1α) does not necessarily prevent moderate and severe autoinflammatory disease.

Acknowledgments

We thank Susanne Ruß, Diana Paul, and Kathrin Höhne for excellent technical assistance, Jürg Tschopp and Gabriel Nunez for kindly providing plasmids, and Andrea Groß for excellent graphic design.

Disclosure Statement: The authors report no conflict of interest.

References

Calligaris L, Marchetti F, Tommasini A, Ventura A. 2008. The efficacy of anakinra in an adolescent with colchicine-resistant familial Mediterranean fever. Eur J Pediatr 167:695–696.

DeLano WL. 2002. Unraveling hot spots in binding interfaces: progress and challenges. Curr Opin Struct Biol 12:14–20.

Dinarello CA. 2005. Interleukin-1beta. Crit Care Med 33:S460-S462.

Dinarello CA. 2011. A clinical perspective of IL-1beta as the gatekeeper of inflammation. Eur J Immunol 41:1203–1217.

Engh R, Huber R. (1991). Accurate bond and angle parameters for X-ray protein structure refinement. Acta Crystallogr. A 47:392–400.

Eswar N, Webb B, Marti-Renom MA, Madhusudhan MS, Eramian D, Shen MY, Pieper U, Sali A. 2007. Comparative protein structure modeling using MODELLER. Curr Protoc Protein Sci Chapter 2:Unit 2.9.

Fahr BT, O'Brien T, Pham P, Waal ND, Baskaran S, Raimundo BC, Lam JW, Sopko MM, Purkey HE, Romanowski MJ. 2006. Tethering identifies fragment that yields potent inhibitors of human caspase-1. Bioorg Med Chem Lett 16:559–562.

Fantuzzi G, Dinarello CA. 1999. Interleukin-18 and interleukin-1 beta: two cytokine substrates for ICE (caspase-1). J Clin Immunol 19:1–11.

Franchi L, Kanneganti TD, Dubyak GR, Nunez G. 2007. Differential Requirement of P2×7 Receptor and Intracellular K+ for Caspase-1 Activation Induced by Intracellular and Extracellular Bacteria. J Biol Chem 282:18810–18818.

Hawkins PN, Lachmann HJ, McDermott MF. 2003. Interleukin-1-receptor antagonist in the Muckle–Wells syndrome. N Engl J Med 348:2583–2584.

Jones TA, Zou JY, Cowan SW, Kjeldgaard M. 1991. Improved methods for building protein models in electron density maps and the location of errors in these models. Acta Crystallogr A 47(Pt 2):110–119.

Kanneganti TD, Body-Malapel M, Amer A, Park JH, Whitfield J, Franchi L, Taraporewala ZF, Miller D, Patton JT, Inohara N, Nunez G. 2006a. Critical role for Cryopyrin/Nalp3 in activation of caspase-1 in response to viral infection and double-stranded RNA. J Biol Chem 281:36560–36568.

Kanneganti TD, Ozoren N, Body-Malapel M, Amer A, Park JH, Franchi L, Whitfield J, Barchet W, Colonna M, Vandenabeele P, Bertin J, Coyle A, Grant EP, Akira S, Nunez G. 2006b. Bacterial RNA and small antiviral compounds activate caspase-1 through cryopyrin/Nalp3. Nature 440:233–236.

Keller M, Ruegg A, Werner S, Beer HD. 2008. Active caspase-1 is a regulator of unconventional protein secretion. Cell 132:818–831.

Kuemmerle-Deschner JB, Ramos E, Blank N, Roesler J, Felix SD, Jung T, Stricker K, Chakraborty A, Tannenbaum S, Wright AM, Rordorf C. 2011. Canakinumab (ACZ885, a fully human IgG1 anti-IL-1beta mAb) induces sustained remission in pediatric patients with cryopyrin-associated periodic syndrome (CAPS). Arthritis Res Ther 13:R34.

Kutzner C, van der SD, Fechner M, Lindahl E, Schmitt UW, de Groot BL, Grubmuller H. 2007. Speeding up parallel GROMACS on high-latency networks. J Comput Chem 28:2075–2084.

Lamkanfi M, Kalai M, Saelens X, Declercq W, Vandenabeele P. 2004. Caspase-1 activates nuclear factor of the kappa-enhancer in B cells independently of its enzymatic activity. J Biol Chem 279:24785–24793.

Laskowski RA, MacArthur MW, Moss DS, Thornton JM. 1993. *PROCHECK*: a program to check the stereochemical quality of protein structures. J Appl Crystallogr D 26:283–291.

Laskowski RA, Moss DS, Thornton JM. 1993. Main-chain bond lengths and bond angles in protein structures. J Mol Biol 231:1049–1067.

Mankan AK, Dau T, Jenne D, Hornung V. 2011. The NLRP3/ASC/Caspase-1 axis regulates IL-1beta processing in neutrophils. Eur J Immunol.

Martinon F, Burns K, Tschopp J. 2002. The inflammasome: a molecular platform triggering activation of inflammatory caspases and processing of proIL-beta. Mol Cell 10:417–426.

Martinon F, Petrilli V, Mayor A, Tardivel A, Tschopp J. 2006. Gout-associated uric acid crystals activate the NALP3 inflammasome. Nature 440:237–241.

Martinon F, Tschopp J. 2004. Inflammatory caspases: linking an intracellular innate immune system to autoinflammatory diseases. Cell 117:561–574.

McDermott MF. 2004. A common pathway in periodic fever syndromes. Trends Immunol 25:457–460.

Murshudov GN, Vagin AA, Dodson EJ. 1997. Refinement of macromolecular structures by the maximum-likelihood method. Acta Crystallogr D 53:240–255.

Murshudov GN, Vagin AA, Lebedev A, Wilson KS, Dodson EJ. 1999. Efficient anisotropic refinement of macromolecular structures using FFT. Acta Crystallogr D 55:247–255.

O'Brien T, Fahr BT, Sopko MM, Lam JW, Waal ND, Raimundo BC, Purkey HE, Pham P, Romanowski MJ. 2005. Structural analysis of caspase-1 inhibitors derived from Tethering. Acta Crystallograph Sect F 61:451–458.

Oostenbrink C, Villa A, Mark AE, van Gunsteren WF. 2004. A biomolecular force field based on the free enthalpy of hydration and solvation: the GROMOS force-field parameter sets 53A5 and 53A6. J Comput Chem 25:1656–1676.

Pannu NS, Murshudov GN, Dodson EJ, Read RJ. 1998. Incorporation of prior phase information strengthens maximum-likelihood structure refinement. Acta Crystallogr D 54:1285–1294.

Petrilli V, Papin S, Dostert C, Mayor A, Martinon F, Tschopp J. 2007. Activation of the NALP3 inflammasome is triggered by low intracellular potassium concentration. Cell Death Differ 14:1583–1589.

Pflugrath JW. 1999. The finer things in X-ray diffraction data collection. Acta Crystallogr D 55:1718–1725.

Ramage P, Cheneval D, Chvei M, Graff P, Hemmig R, Heng R, Kocher HP, Mackenzie A, Memmert K, Revesz L. 1995. Expression, refolding, and autocatalytic proteolytic processing of the interleukin-1 beta-converting enzyme precursor. J Biol Chem 270:9378–9383.

Raupach B, Peuschel SK, Monack DM, Zychlinsky A. 2006. Caspase-1-mediated activation of interleukin-1beta (IL-1beta) and IL-18 contributes to innate immune defenses against *Salmonella enterica* serovar Typhimurium infection. Infect Immun 74:4922–4926.

Romanowski MJ, Scheer JM, O'Brien T, McDowell RS. 2004. Crystal structures of a ligand-free and malonate-bound human caspase-1: implications for the mechanism of substrate binding. Structure 12:1361–1371.

Sali A, Blundell TL. 1993. Comparative protein modelling by satisfaction of spatial restraints. J Mol Biol 234:779–815.

Scheer JM, Romanowski MJ, Wells JA. 2006. A common allosteric site and mechanism in caspases. Proc Natl Acad Sci USA 103:7595–7600.

Scheer JM, Wells JA, Romanowski MJ. 2005. Malonate-assisted purification of human caspases. Protein Expr Purif 41:148–153.

Shen MY, Sali A. 2006. Statistical potential for assessment and prediction of protein structures. Protein Sci 15:2507–2524.

Simon A, Bodar EJ, van der Hilst JC, van der Meer JW, Fiselier TJ, Cuppen MP, Drenth JP. 2004. Beneficial response to interleukin 1 receptor antagonist in traps. Am J Med 117:208–210.

Sutterwala FS, Ogura Y, Szczepanik M, Lara-Tejero M, Lichtenberger GS, Grant EP, Bertin J, Coyle AJ, Galan JE, Askenase PW, Flavell RA. 2006. Critical role for NALP3/CIAS1/Cryopyrin in innate and adaptive immunity through its regulation of caspase-1. Immunity 24:317–327.

Vagin AA, Teplyakov A. 1997. MOLREP: an Automated Program for Molecular Replacement. J Appl Cryst 30:1022–1025.

Vaguine AA, Richelle J, Wodak SJ. 1999. *SFCHECK*: a unified set of procedures for evaluating the quality of macromolecular structure-factor data and their agreement with the atomic model. Acta Crystallogr D 55:191–205.

van Gunsteren WF, Berendsen HJ, Hermans J, Hol WG, Postma JP. 1983. Computer simulation of the dynamics of hydrated protein crystals and its comparison with x-ray data. Proc Natl Acad Sci USA 80:4315–4319.

Walker NP, Talanian RV, Brady KD, Dang LC, Bump NJ, Ferenz CR, Franklin S, Ghayur T, Hackett MC, Hammill LD, Herzog L, Hugunin M, Houy W, Mankovich JA, McGuiness L, Orlewicz E, Paskind M, Pratt A, Reis P, Summani A, Terranova M, Welch JP, Xiong L, Möller A, Tracey DE, Kamen R, Wong WW. 1994. Crystal structure of the cysteine protease interleukin-1 beta-converting enzyme: a (p20/p10)2 homodimer. Cell 78:343–352.